



OBSERVATIONS AND MODELLING OF THE PROCESSING OF AEROSOL BY A HILL CAP CLOUD

K. N. BOWER,* T. W. CHOULARTON,* M. W. GALLAGHER,*
 R. N. COLVILE,* M. WELLS,* K. M. BESWICK,* A. WIEDENSOHLER,†‡
 H-C. HANSSON,†§ B. SVENNINGSSON,† E. SWIETLICKI,† M. WENDISCH,¶
 A. BERNER,|| C. KRUISZ,|| P. LAJ,** M. C. FACCHINI,** S. FUZZI,**
 M. BIZJAK,†† G. DOLLARD,‡‡ B. JONES,‡‡ K. ACKER,§§¶¶
 W. WIEPRECHT,§§¶¶ M. PREISS,|| M. A. SUTTON,***
 K. J. HARGREAVES,*** R. L. STORETON-WEST,*** J. N. CAPE***
 and B. G. ARENDS†††

*Physics Department, UMIST, P.O. Box 88, Manchester M60 1QD, U.K.; †Division of Nuclear Physics, Lund University, Sölvegatan 14, S-22362 Lund, Sweden; ‡Institute for Tropospheric Research, Permoserstrasse 15, D-04303 Leipzig, Germany; ¶Institut für Experimentalphysik, Universität Wien, Strudlhofgasse 4, A-1090 Wien, Austria; **Istituto FISBAT -C.N.R., Via Gobetti 101, 40129 Bologna, Italy; ††National Institut of Chemistry, Hajdrihova 19, 61115 Ljubljana, Slovenia; ‡‡AEA Technology, National Environment Technology Centre, Culham, Abingdon, Oxon OX14 3DB, U.K.; §§Fraunhofer Institut für Atmosphärische Umweltforschung, Aussenstelle für Luftchemie, Rudower Chaussee 5, D-12484 Berlin, Germany; ||Zentrum für Umweltforschung, Universität Frankfurt, Georg Voigt Strasse 14, D-60325 Frankfurt, Germany; ***Institute of Terrestrial Ecology, Edinburgh Research Station, Bush Estate, Penicuik EH26 0QB, U.K.; and †††Netherlands Energy Research Foundation, P.O. Box 1, 1755 ZG, The Netherlands

(First received 7 November 1995 and in final form 18 October 1996. Published May 1997)

Abstract—Observations are presented of the aerosol size distribution both upwind and downwind of the Great Dun Fell cap cloud. Simultaneous measurements of the cloud microphysics and cloud chemistry, and of the chemical composition of the aerosol both upwind and downwind of the hill were made along with measurements of sulphur dioxide, hydrogen peroxide and ozone. These observations are used for initialisation of, and for comparison with the predictions of a model of the air flow, cloud microphysics and cloud chemistry of the system.

A broad droplet size distribution is often observed near to the hill summit, seemingly produced as a result of a complex supersaturation profile and by mixing between parcels with different ascent trajectories. The model generates several supersaturation peaks as the airstream ascends over the complex terrain, activating increasing numbers of droplets. In conditions where sulphate production in-cloud (due to the oxidation of S(IV) by hydrogen peroxide and ozone) is observed, there is a marked effect on the chemical evolution of the aerosol particles on which the droplets form.

When sulphate production occurs, a significant modification of the aerosol size distribution and hygroscopic properties is both predicted and observed. The addition of sulphate mass to those aerosol particles nucleation scavenged by the cloud generally increases the ease with which they are subsequently able to act as cloud condensation nuclei (CCN). Often, this will lead to an increase in the number of CCN available for subsequent cloud formation, although this latter effect is shown to be strongly dependent upon the activation history of the droplets and the concentration of pollutant gases present in the interstitial air. Situations are also identified where cloud processing could lead to a reduction in the capacity of smaller aerosol to act as CCN. © 1997 Elsevier Science Ltd.

Key word index: Aerosol modification, accumulation mode, CCN, nucleation scavenging, cloud microphysics, cloud chemistry, S(IV) oxidation, cap cloud model.

1. INTRODUCTION

Atmospheric aerosols affect climate through the influence they have on the Earth's radiation budget. They have both a direct effect by scattering incoming solar radiation and an indirect effect via the role they play as cloud condensation nuclei (CCN). In this latter

‡Now at: Institute for Tropospheric Research, Permoserstrasse 15, D-04303 Leipzig, Germany.

§Now at: Department of Meteorology, Stockholm University, S-10691 Stockholm, Sweden.

¶¶Now at: Brandenburgische Technische Universität Cottbus, Lehrstuhl Luftchemie und Luftreinhaltung, AG Luftchemie, Rudower Chaussee 5, D-12484 Berlin, Germany.

role, aerosols control the number of droplets which activate within a given cloud system. This in turn controls the droplet effective radius for a given liquid water content and hence the albedo of the cloud (see Slingo, 1990 for a discussion of the sensitivity of the radiative properties of clouds to changes in the droplet effective radius). Depending upon the cloud type, the efficiency of precipitation development and hence cloud lifetime may also be affected by changes in cloud drop sizes (Bower and Choulaton, 1993) and so changes in CCN activities may also affect the extent and longevity of cloud cover.

The natural aerosol has been substantially perturbed by anthropogenic aerosol in recent times, for example, by sulphates formed from SO₂ emissions. The global mean radiative forcing due to the direct radiative effect of anthropogenic aerosols has been calculated to be of a similar magnitude but opposite sign to the radiative forcing of anthropogenic greenhouse gases (Charlson, 1992). The indirect effect is poorly quantified but may be at least as important as the direct effect. Despite their importance, the effects of aerosol particles are still very poorly represented in global climate models. This is due partly to a lack of globally distributed data sets, but it is also due to the absence of a clear understanding of the chemical processes linking gaseous precursor emissions (e.g. sulphur compounds and oxides of nitrogen) to the size distribution and hygroscopic properties of aerosol, aerosol optical depth and cloud reflectivity.

Observational studies of the processing of aerosols by cloud (e.g. Hoppel *et al.*, 1994) have demonstrated that a bimodal aerosol size distribution is often produced. Modelling studies (e.g. Bower and Choulaton, 1993) have also predicted that cloud processing will lead to a bimodal aerosol size distribution and that this will enhance the number of CCN available for subsequent cloud formation.

As part of the GCE experiment performed in 1993 at Great Dun Fell (GDF), in Cumbria, England, an experiment was designed to investigate the influence of a single passage through cloud on the size distribution and chemical composition of the atmospheric aerosol. These measurements were performed as part of a larger and detailed investigation of the chemical and microphysical processes occurring within the cap cloud system. This was the first time that it was possible to carry out such a complete investigation of the processing of aerosols by cloud, the collaborative experiment enabling a comprehensive set of aerosol measurements to be made along with the required chemical and microphysical measurements at multiple sites along a single transect through a well-defined cloud system.

In this paper, measurements of the dry aerosol size spectrum in the size range 7–600 nm at Moor House (MH) (upwind of the GDF cap cloud in all the case studies considered) and in the size range 3–600 nm at the Fell Gate (FG) site (downwind of the cap cloud) are presented and compared for four case study

periods. Changes in the spectral shape, particularly in the accumulation mode size range (approximately 100–300 nm) and at the upper end of the Aitken mode (20–100 nm), which are likely to have been brought about by processing of the aerosol within the cap cloud are then examined by means of a Lagrangian cloud parcel model. This considers both the microphysical and chemical development of the aerosol population as the particles are nucleation scavenged into cloud droplets.

A full description of the measurement sites and of the instruments operated at each of the sites in the 1993 GCE experiment held at GDF is presented in the outline paper of Choulaton *et al.* (1997). The aerosol size distributions considered were all measured by Differential Mobility Particle Sizer instruments (DMPSs). A detailed description of these instruments and their operation at GDF is provided by Wiedensohler *et al.* (1997). An outline of the combined cloud microphysics and cloud chemistry model used in this study is provided in Section 2. In Section 3, the observed aerosol spectra upwind and downwind of the cap cloud system are considered and compared to the changes predicted by the model. Model and observed cloud microphysical properties are also presented. Finally, the results of aerosol processing within cloud and their wider implications are discussed in Section 4.

2. THE AEROSOL-PROCESSING MODEL

The UMIST cap cloud chemistry model (Hill *et al.*, 1986; Bower *et al.*, 1991; Colvile *et al.*, 1994) was used. This model considers the nucleation scavenging and subsequent microphysical and chemical development of an explicit input aerosol distribution, initially in equilibrium at 99% relative humidity, as the air parcel in which they reside is forced to flow up and over the complex terrain, which in this case describes the north Pennine ridge of which GDF forms a part.

The Lagrangian microphysics and chemistry model used is essentially that described by Bower *et al.* (1991). It requires dynamical input (updraughts and horizontal wind speeds) as a function of position, which it obtains from a look-up table generated by an air flow model. In this work, output from the air flow model FLOWSTAR was used. The air flow modelling for each of the case studies is described in detail by Wobrock *et al.* (1997) and will not be discussed further.

The microphysical model used is a development of that presented by Bower and Choulaton (1988), and is based upon a standard one-dimensional (1D) adiabatic growth model as described by many authors (e.g. Pruppacher and Klett, 1978). Starting at cloud base, a representative CCN spectrum of mixed origin (which is usually based upon the soluble mass components of a measured aerosol size distribution as described below) initially at 99% relative humidity, is

allowed to develop adiabatically until the parcel in which they reside exits the cloud or arrives at an observation site within the cloud. The equations are solved using a forward differencing technique. The model is modified to take account of the effects of homogeneous dry air entrainment near to cloud top either as described by Bower *et al.* (1991), or as used in this work by a simple addition of heat and H_2O_2 into the cloud parcel from above. For the latter, the temperature of the entrained air was determined from the Boulmer soundings (see overview paper, Choulaton *et al.*, 1997) and the H_2O_2 mixing ratio was estimated from measurements made at the summit during periods in the campaign when there was no cloud.

2.1. The input aerosol spectrum

The input spectrum used in the model was deduced from log-normal fits to the upwind size distribution of the aerosol measured by the DMPS system (upper cut-off 600 nm). These measurements provide nearly 100% of the aerosol particles by number, but when compared to impactor measurements of aerosol mass (bulk soluble mass from the Rotheroe–Mitchell device, upper cut-off $\sim 40 \mu\text{m}$), or to total nucleation scavenged ion loadings (from cloud-water analysis, effectively infinite upper CCN cut-off) can account for as little as 40% of the total aerosol mass. As re-partitioning of certain species making up the soluble component of aerosol mass can occur between aerosols of different size and composition in-cloud, it is important to take account of the missing soluble mass in the model input. This was done by fitting an additional log-normal mode of dry diameter around $1 \mu\text{m}$ (mass mode wet diameter around $3 \mu\text{m}$) to the DMPS spectra. These mass modes contain few particles by number and so were often not detected by the particle counting techniques employed in this experiment. The calculated input spectra were then checked against size-segregated aerosol chemistry measurements (made by four-stage Berner impactors, with upper cut-offs of 5, 1.4, 0.36 and $0.1 \mu\text{m}$), and also compared with aerosol size distributions measured by optical particle counters (over 32 channels, $0.1\text{--}3 \mu\text{m}$). Due to persistent instrument problems, the latter measurements were often unreliable and so were not used quantitatively.

Data from the Tandem Differential Mobility Analyzer (TDMA) operated at Fell Gate were used to determine the fractions of insoluble material present in the aerosol at a given size. It was assumed that this material was conserved on passage through the cloud and that it played no role in either the chemistry or microphysics of the system (other than to increase the volume of the particles). Svenningsson *et al.* (1997) report that aerosols at GDF were often composed of an external mixture of particles with high and low insoluble fractions at each size. The log-normal distributions in both the Aitken (AK) and Accumulation (AC) modes were thus divided up into

a more hygroscopic and a less hygroscopic distribution (to reflect this external mixture when observed). For the purpose of this modelling exercise, only the more soluble AK and AC modes, the less soluble AC mode and the additional coarse mode have been included. Most particles in the less soluble AK mode would not be nucleation-scavenged into cloud droplets and so have been omitted from the model input. However, to compare model predictions of modifications directly with the observed spectra before and after cloud processing, this mode would need to be included.

The internal mixture of soluble components of the aerosol at each size was obtained by relating the soluble fraction of the total aerosol volume in each mode, to the bulk soluble aerosol mass loadings. These data were derived from a combination of the integrated multistage Berner impactor measurements and the bulk filter Rotheroe–Mitchell measurements (see Choulaton *et al.*, 1997). The speciation of the soluble mass within each mode was thus set constant at all sizes within each mode, and was the same for all modes except the additional coarse mode, the size of which was adjusted to carry the remaining soluble mass. All observed loadings of sodium and most of chloride were placed into the mass mode when present. Small amounts of the chloride were used within the other modes to obtain near charge neutrality at input (and hence a realistic cloud droplet pH). All cloud-water nitrate was also included in the input aerosol as no independent measurement of $\text{HNO}_{3(g)}$ was available at MH.

The size-resolved chemical composition measurements made by the multistage Berner impactors were used to check whether the mass loadings and speciation of soluble components within modes were realistic. This was achieved by rebinning the wet parameterised spectrum according to the cut sizes of the impactor stages. On most occasions there was good agreement, and a realistically sized mass mode was produced. On other occasions the dispersion of the log-normal accumulation mode had to be increased by about 10% in order to be consistent with the variation in mass and speciation between the impactor stages, and so as not to require an unrealistically large mass mode.

Finally, the continuous aerosol spectrum and its associated properties (determined as above) was divided back up into a finite number of discrete size bins for input to the cloud model. For each bin, all particles have to assume the volume-weighted mean diameter of that bin, since the use of any other weighted mean will result in a large error in the total aerosol mass. However, the droplet growth equation contains terms of order D (diameter) as well as D^3 . In order to model the GDF system, it was therefore necessary to have the particle size bins sufficiently small so that the use of the volume mean diameter (as opposed to the number mean diameter) represented a systematic error that was smaller than the

uncertainty in the corresponding measurements. It was found that a minimum of ten bins per decade of particle size (producing an upper bin delimiter 1.25 times larger than the lower bin delimiter) produced a systematic size error of less than 10%. The equilibrium (wet) aerosol size distributions input to the model were then calculated using the Köhler equation as described in Bower and Choulaton (1993).

2.2. The Cap Cloud Chemistry Model

The chemistry model used is essentially that of Bower *et al.* (1991) modified to include the extended chemistry scheme of Sander *et al.* (1995). The reader is referred to these papers for the details of the chemistry scheme and the rate constants employed. The model considers the oxidation of aqueous sulphur (IV) species within individual cloud drops by reaction with the dissolved oxidants ozone and hydrogen peroxide, and iron (III) catalysed O_2 . The inhibiting effect of formaldehyde is now included, but is found to have a negligible effect in the cases considered. The formation of nitric acid in solution via the nighttime formation of higher oxides of nitrogen in the gas phase is also included in this version of the model, but again this pathway does not contribute significantly to the formation of aerosol soluble mass in the case studies investigated here. It will, however, be important in other conditions.

The chemical system includes the gases H_2O_2 , O_2 , O_3 , SO_2 , formaldehyde, NH_3 , NO , NO_2 , NO_3 , N_2O_5 , HNO_2 , HNO_3 and CO_2 , the solubility of which in cloud-water drops is determined by the Henry's law solubility constants. Both solubility and the subsequent dissociation constants (Sander *et al.*, 1995) are calculated at the input cloud base temperature. In this model, only the gases ozone and carbon dioxide are assumed always to be in equilibrium. All other gases including SO_2 are assumed to be taken up by the individual cloud droplets at a finite rate, and may not therefore be in equilibrium at all times.

The chemistry model is activated only when the integrated liquid water content L , of the cap cloud parcel, calculated in the microphysical model, exceeds 0.01 gm^{-3} . This generally occurs within around 10 m of cloud base in the standard model, after about 5 s development time. The condition is applied in order to avoid having to model the highly complex interactions which occur between ions at very high concentrations in non-ideal solutions, and which are extant for a short period only. In the same way, only droplets larger than $0.5 \mu\text{m}$ are allowed to participate in active chemistry (even when $L > 0.01 \text{ gm}^{-3}$), although concentration changes of species resulting from changes in drop sizes are calculated for all droplets.

Following each call to the chemistry routine, the new "effective" CCN mass within each droplet category is calculated. Only the ions Na^+ , NH_4^+ , Cl^- ,

SO_4^{2-} , NO_3^- , and a charge balancing fraction of H^+ or OH^- ions are considered to contribute to the soluble CCN mass, since these are the dominant ions observed in the measured aerosol at GDF (Laj *et al.*, 1997) and are the ions which are present in the input distributions.

The model runs are terminated when the parcel liquid water content falls below 0.01 gm^{-3} for the last time. Since the current model is unable to consider the more complex chemistry occurring within the evaporating cloud droplets as they return to the unactivated aerosol phase, the concentrations of ions forming the new soluble CCN mass is assumed to remain fixed. The output dry aerosol size distribution is then reconstructed by converting the particles to their dry size and assuming no further exchange with the environment occurs. The insoluble volume within each aerosol category, carried as an inert parameter throughout the model development, is also incorporated. The predicted aerosol modification may then be compared with the measured aerosol spectrum following passage through the cap cloud.

The validity of assuming no further exchange occurs between evaporating cloud drops and the atmosphere below $L = 0.01 \text{ gm}^{-3}$ has been tested by a number of methods. Firstly, the effect of freezing the droplet sizes at $L = 0.01 \text{ gm}^{-3}$ and allowing equilibrium to be established between species in the aqueous and gaseous phases, produced negligible changes in the final CCN masses. Allowing the same process to occur within droplets reduced to their equilibrium size at 99% relative humidity (i.e. by assuming low ionic strength chemistry could be applied to the unactivated aerosol) produced more outgassing of volatile CCN species, but still insufficient to change significantly the new dry aerosol size distribution.

Preliminary work using a more detailed model which considers the effects of high ionic strength on the effective concentrations of species within aerosols, suggests significant outgassing of species such as NH_3 , HCl and HNO_3 might occur from different droplets (in the absence/presence of significant sulphate production in the case of NH_3/HCl or HNO_3 , respectively) or in conditions where ambient concentrations of these species in the atmosphere are low. This would certainly invalidate the assumption made in this work. However, these observations suggest that significant outgassing would also occur from the input aerosol distributions used. This implies that the degree of outgassing must be limited kinetically and/or by the time spent at humidities above the deliquescence point of the various CCN constituents. We suggest, therefore, that this effect will not significantly change the predicted size distributions or the increase in the soluble mass of the particles for the case studies presented in this paper (which are dominated primarily by sulphate production). The outgassing of ammonia from the cloud processed aerosol is discussed in detail in Wells *et al.* (1997).

3. OBSERVATIONS AND COMPARISON WITH MODEL PREDICTIONS

Four periods have been chosen for detailed investigation. These were selected on the basis that they represent a considerable variation in the prevailing conditions such as cloud base height, oxidant concentrations, sulphur dioxide concentrations, etc., and because the majority of measurements required for input to the model were available. The periods chosen are shown in Table 1. The run numbers refer to model case studies and not to the periods of intensive measurements that are described in other papers.

The comprehensive suite of measurements carried out at GDF are described in detail in the overview paper (Choularton *et al.*, 1997). Most of the measurements made at the five sites were used either as input to the cloud processing model, or for comparison with its microphysical and chemical predictions. For each of the case studies presented the air flow was from NE to SW. Moor House (MH) was, therefore, the only upwind site on each of these occasions. Periods when it was affected by cloud are discussed by Colvile *et al.* (1997).

The aerosol size distributions, soluble fractions and chemical composition, prepared from the observations and input to the model were accompanied by trace gas inputs that were directly measured outside of cloud. The exceptions are hydrogen peroxide and nitric acid, as no upwind gas-phase measurements were available for these case studies. For model runs in which entrainment was assumed to be negligible, the upstream H₂O₂ input was set so as to reproduce the observed aqueous-phase concentrations at the summit (SU) (and Mine Road (MR), when measurements were available), taking into account the reduction processes occurring between cloud base and summit. When entrainment was occurring, an entrained gas-phase concentration was assumed which reproduced the observed aqueous-phase concentration at MR, since no measurements were available above the cloud. It was assumed that the aqueous-phase hydrogen peroxide observed at SU had entered through cloud base since previous detailed studies (e.g. Gallagher *et al.*, 1991) suggest that entrained air does not substantially penetrate to the hill surface until downwind of the summit. This is supported by the thermodynamic data for the case studies presented (Colvile *et al.*, 1997; Wobrock *et al.*, 1997). Colvile *et al.* (1997) provide a detailed table of the periods affected by entrainment during the 1993 experiment. In this

Table 1. The case study periods investigated in this paper

Date	Time (BST)	Run number	Code
9 May	18:00–22:00	Run 5	05091822
10 May	02:00–04:00	Run 6	05100204
10 May	19:00–21:00	Run 8	05101921
10 May	22:30–23:30	Run 9	05102323

study, only runs 8 and 9 are considered to be strongly affected by entrainment.

Table 2 summarises the concentrations of the major gas-phase species that were observed and input to the model for each of the case studies. It can be seen that runs 5 and 6 are clean with relatively little SO₂ (about 0.2 ppbv), whereas runs 8 and 9 have SO₂ concentrations of 4 and 6 ppbv respectively. Tropospheric concentrations of peroxide, for case studies 8 and 9 (affected by entrainment) were determined as described above. For a detailed discussion of the meteorological conditions prevailing during the case studies, the reader is referred to the paper of Colvile *et al.* (1997).

Various aspects of the development of the cloud microphysics and aerosol processing will now be considered in detail on a subject by subject basis. Where possible, a comparison between model and observations will be made, as well as a comparison between the individual case studies.

3.1. Cloud microphysical development

Table 3 shows the summit liquid water contents and droplet number concentrations averaged over the duration of each of the case studies compared with the model predictions. Two model runs were carried out for runs 8 and 9, one considering development within a standard closed cloud parcel and the other considering the effects of entraining heat and fresh H₂O₂ into the cloud from the free troposphere above. Since the major effects of entrainment are generally only observed downwind of the summit, the simple entrainment scheme employed in the model was activated

Table 2. The principal gas-phase measurements (in ppbV) input to the model for the four case studies

Run no.	SO ₂	H ₂ O ₂	O ₃	NH ₃	H ₂ O ₂ entrained
5	0.2	0.2	45.0	0.3	0.0
6	0.2	0.15	40.0	0.14	0.0
8	4.0	1.0	45.0	0.2	0.0
8B	4.0	0.0	45.0	0.2	5.0
9	6.0	1.0	50.0	0.5	0.0
9B	6.0	0.0	50.0	0.5	5.0

Table 3. The observed and predicted cloud droplet number and liquid water contents at the SU site for the four case studies

Run no.	Liquid water content (mg m ⁻³)		Droplet number (cm ⁻³)	
	Observed	Modelled	Observed	Modelled
5	473	495	535	648
6	630	537	482	1121/978
8	819	762	540	765/479
9	592	485	549	908/780

Note: Two values of modelled droplet number indicate two nearest values to summit.

only following arrival at the summit. Only one set of results is therefore presented for SU in Table 3 for runs 8 and 9.

In general, good agreement exists between the summit microphysical properties and the observed cloud structure. Exceptions to this include the modelled cloud droplet concentrations which on the whole tend to be too large (particularly in case studies 6 and 9). A possible cause of this discrepancy might have been the use of too small a condensation coefficient α_c , in the microphysics model. A value of 0.035 was originally used, an average obtained from several measurements carried out over pure water surfaces (see Table 5.4, Pruppacher and Klett, 1978). This value was increased to 0.1 in this work, in line with recent modelling activities which suggest a value closer to unity may be more appropriate for polluted aerosol. A sensitivity test was carried out to examine the effect of further increasing α_c in these case studies (where complicated activation histories are predicted as described below). Although the initial activated drop number was reduced (by increasing α_c), this was generally offset subsequently by additional activation in later supersaturation peaks which were larger (than in lower α_c cases) generating a similar final droplet number at cloud top. The source of the discrepancy in cloud droplet number is thus more likely to be due to a combination of effects, including the inability of any simple 1D parcel model to take account of the effects of variations in humidity, updraught and mixing experienced by air parcels before, during and following activation at cloud base (which itself is often variable). In addition, some of the less-soluble material internally mixed within aerosols (and treated as inactive material within this study) may be playing an active role during nucleation scavenging, affecting the rate of growth of drops (by its gradual dissolution and by changing the drops surface tension e.g. Shulman *et al.*, 1996). This will require further investigation in the field and laboratory to ascertain the composition and effects of this material, as well as further modelling studies.

Discrepancies in SU liquid water contents L (Table 3) suggest errors in the specified cloud base altitudes of +11, -47, -29 and -53 m (for cases 5, 6, 8 and 9, respectively). Looking at the time taken to ascend these distances from the prescribed cloud bases, this represents an additional -2, +7 (ignoring the initial brief activation burst in case 6) +14 and +8% of the total reaction time available. This should not significantly affect the overall aerosol modification predicted, and so a closer match has not been attempted. In any case, CB altitudes (suggested by L at SU) are so low that they often lie near to or outside the terrain domain of the air flow model, and so the trajectories predicted for air parcels early on in their history near to cloud base cannot be relied upon with great certainty (particularly if velocity profile has to be specified in order to lift a parcel into the model domain as in cases 8 and 9). Thus, no great benefit can

be obtained in trying to derive more exact replications of observed SU L by adjusting CB, since the differences in modification resulting from this change could not be regarded as being more representative, or better in any way.

Figures 1–4 show the modelled supersaturation histories experienced by the droplets for the four case studies. In each case the altitude of the air parcel is shown together with the profile of droplet number concentration (radius $> 0.5 \mu\text{m}$). It is immediately apparent that as the airstream accelerates up the hill a complex multi-peaked supersaturation history is predicted, which is strongly dependent upon the air parcel trajectory and wind speed.

In cases 5 and 6, with cloud bases near to steep sections of hill, the largest peaks in supersaturation S , occur near to cloud base, so most cloud droplets are activated in this region. In case 6, this number concentration persists until the summit is reached. In case 5, however, the initial high number concentration is reduced during descent from the first steep hill (and subsequent hills). The periods of low supersaturation (or undersaturation) are sufficient to enable evaporation of the smallest drops. In case 6, a brief period of low S also occurs, but this is insufficient for significant evaporation, and so the number of droplets present in the model at SU exceeds the number observed. As the result is highly dependent on air trajectory, an error in this may account for the large discrepancy.

Case study 8 has a lower cloud base than any of the other runs, and so has a higher summit liquid water content. The cloud base (calculated assuming an adiabatic value of liquid water content at the summit) was in fact below the altitude of the first grid point at the edge of the air flow domain. In order to model this case study, wind components at the base of the first hill (some way in from the edge of the domain) were extended back until the cloud base altitude was reached. This produced gentle updraughts near to cloud base with the largest updraughts occurring higher up the hill. The supersaturation near to cloud base was thus considerably lower than the peak occurring later along the trajectory. This resulted in a very broad droplet spectrum in the cloud at the hill summit. Figure 5 shows a comparison between the observed and calculated droplet size distributions at the summit for case 8 (which produced the only modelled spectrum that was broader than the observed—possibly suggesting that the prescribed incline below cloud base was too shallow). In cases 5 and 6, the modelled summit droplet distributions were considerably less broad than the observed, a result which is often obtained when comparing modelled spectra (generated by closed parcel models without mixing) with observations (see Hallberg *et al.*, 1997).

In case study 9, cloud base was also near the edge of the terrain domain, but on this occasion the altitude was encompassed by the wind flow grid. The initial hill gradients are larger than in case 8 and the peak

Run 5 (05091822)

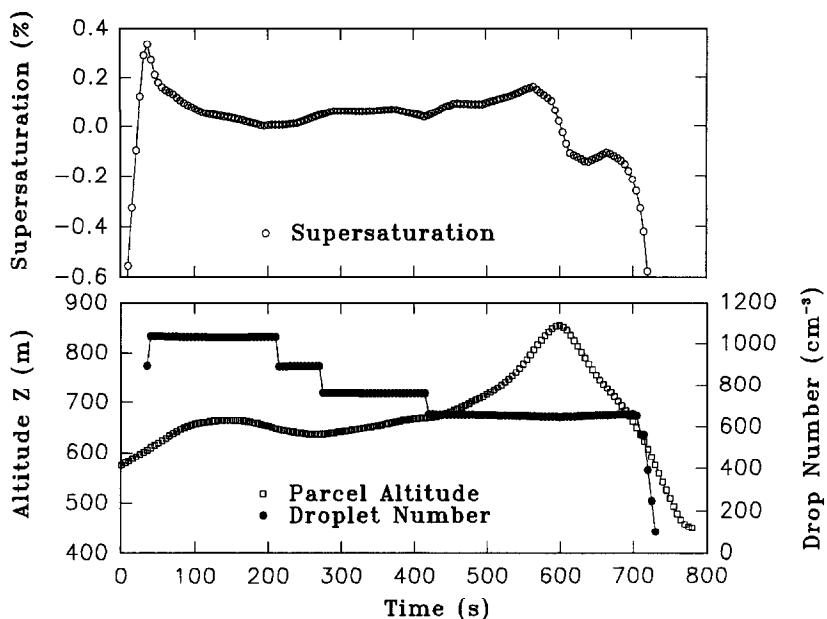


Fig. 1. The time histories of supersaturation, cloud droplet number concentration and cloud parcel altitude for model run 5.

Run 6 (05100204)

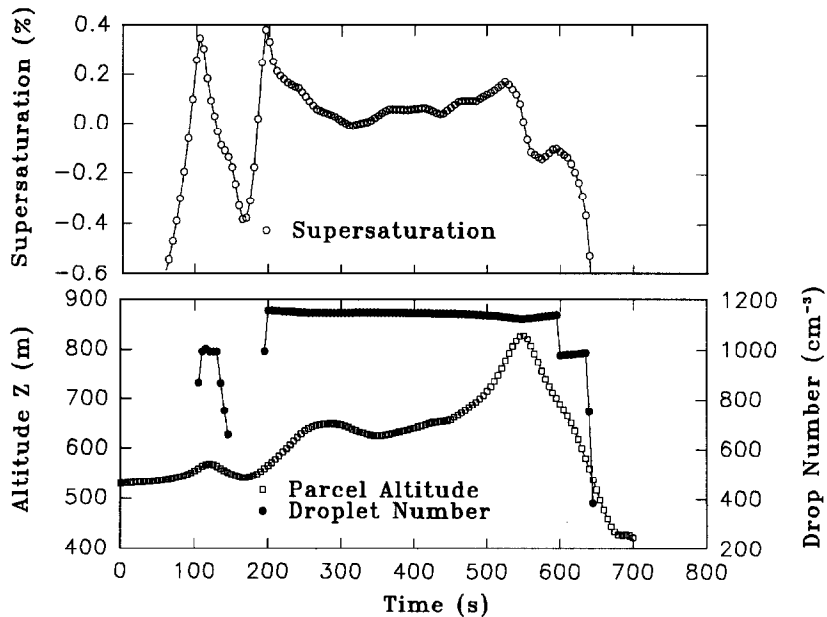


Fig. 2. As Fig. 1 but for model run 6.

supersaturation occurs close to cloud base. The subsequent periods of undersaturation are sufficiently prolonged to enable evaporation of the smallest drops (as in case 5) before reaching the hill summit, although some reactivation occurs just before the summit. In this case the droplet distribution at the summit was

also quite broad, slightly less so than the observed, but (of all the case studies) provided the best agreement with the measurements.

In addition to affecting the microphysical structure of the cloud, the complex activation processes will also have important implications for the chemical

Run 8 (05101921)

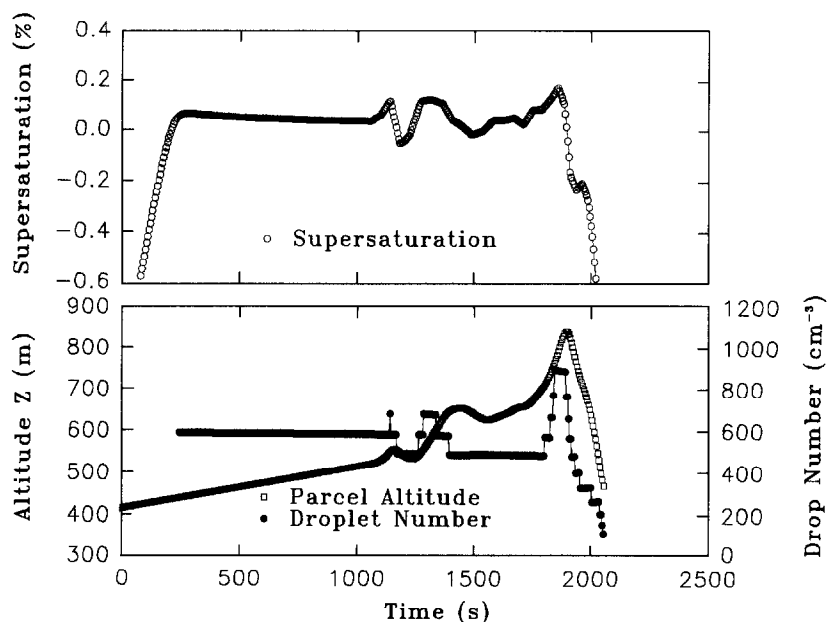


Fig. 3. As Fig. 1 but for model run 8.

Run 9 (05102323)

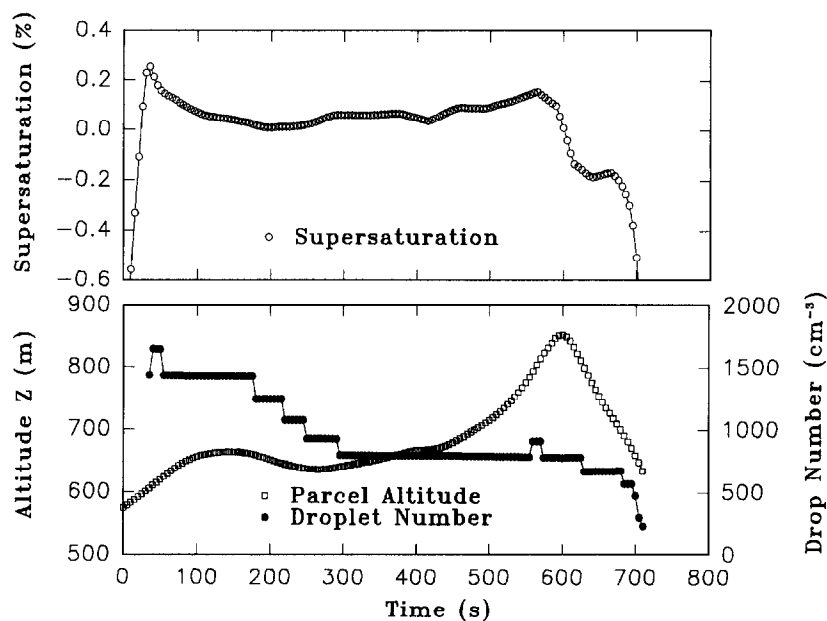


Fig. 4. As Fig. 1 but for model run 9.

transformations which are able to occur within cloud droplets. For example, hydrogen peroxide, the dominant fast acting oxidant, on entering cloud base will tend to be consumed by reaction within the drops

activated in the early stages of cloud formation. If the absolute value of the supersaturation maximum near cloud base is low (e.g. where cloud forms over shallow hills where W is low), then the droplets formed will

Run 8 (05101921)

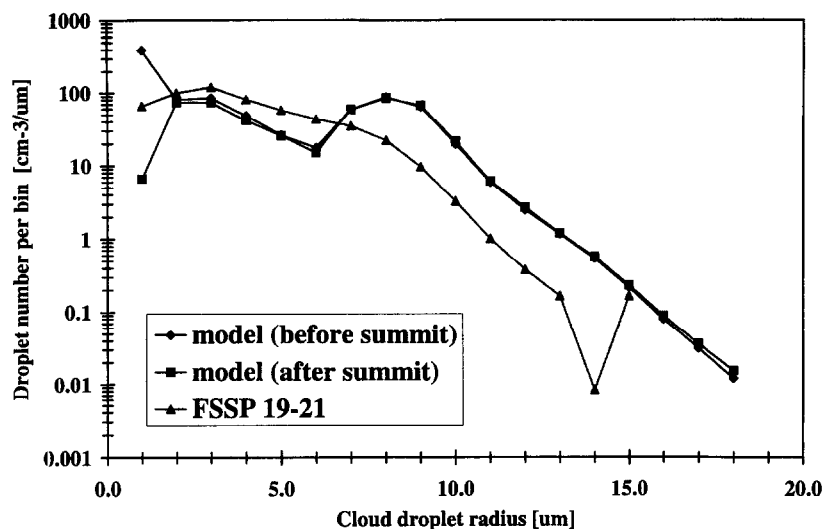


Fig. 5. Observed (FSSP) and predicted cloud droplet spectra at the SU site for case study 8.

activate only on the large aerosol particles with the highest soluble mass. The addition of mass generated by sulphate production to these already large aerosol will have relatively little impact on their subsequent ability to act more efficiently as CCN or on their direct radiative properties. In this case, in order to generate significant aerosol modification a secondary peak in S would need to occur (in order to activate smaller aerosol) and within a time period short compared to the time required to consume the principal reactants (particularly H_2O_2) involved in the S(IV) oxidation reaction. This would enable sulphate production to occur within droplets formed on smaller CCN. These are the aerosol which are most affected by an increase in soluble mass, since a small absolute gain will significantly improve their ability to act subsequently as CCN (and will also dramatically alter their direct radiative properties). A similar modification might be obtained if smaller aerosol were activated later on in the development, prior to the entrainment of hydrogen peroxide through cloud top. Often, however, the peak supersaturation occurs at cloud base allowing (when of sufficient magnitude) activation and modification of the smaller more susceptible CCN early on in the clouds lifetime. In summary, the degree of modification of aerosol properties depends primarily on the magnitude of the supersaturation maximum occurring at cloud base, and if this is relatively low (activating only large aerosol) on the occurrence of a secondary peak close to cloud base or just prior to the entrainment of fresh oxidant into the cloud through cloud top.

3.2. The modification of the aerosol spectrum

Figures 6–9 show a comparison of the log-normal fits to the average DMPS spectra measured at Moor

House and Fell Gate for case studies 5 and 8. In each case, substantial modification of the dry aerosol spectrum at all sizes occurs between the two sites. The changes that occur in the ultrafine nucleation mode size ranges (below around 30 nm) are considered in Wiedensohler *et al.* (1997). Of interest here are the effects of passage through cloud on the aerosol making up the accumulation and upper Aitken modes, i.e. the aerosols that undergo nucleation scavenging to cloud drops. Figures 10–13 show the predicted aerosol modifications in this size range for the four case studies. Model predictions will now be compared with the observed changes for each case.

In case study 5, the modelled spectrum shows little change in the size range 50–600 nm but a significant change is observed. The predicted small change in the accumulation mode is consistent with the low concentrations of SO_2 measured, and used as input on this occasion. The model produces only a $0.05 \mu g m^{-3}$ increase in sulphate over an initial mass loading of $3.0 \mu g m^{-3}$. It is possible that the discrepancy between observed and calculated behaviour is due to the scavenging or production of another ion. However, aerosol chemistry measurements show an increased sulphate loading of $\sim 1.5 \mu g m^{-3}$. Although in disagreement with the measured SO_2 concentrations, this discrepancy could explain much of the observed aerosol size modification, and given higher SO_2 inputs, could be reproduced by the model.

Case study 6 also has low ambient SO_2 concentrations, but rather more modification of the spectral shape at around 100 nm is predicted on this occasion (Fig. 8). This is consistent with the observed modification at this size. The predicted change is produced as a result of sulphate production in the very small particles (less than 100 nm) that are activated by the

May 09, 20:45-22:45

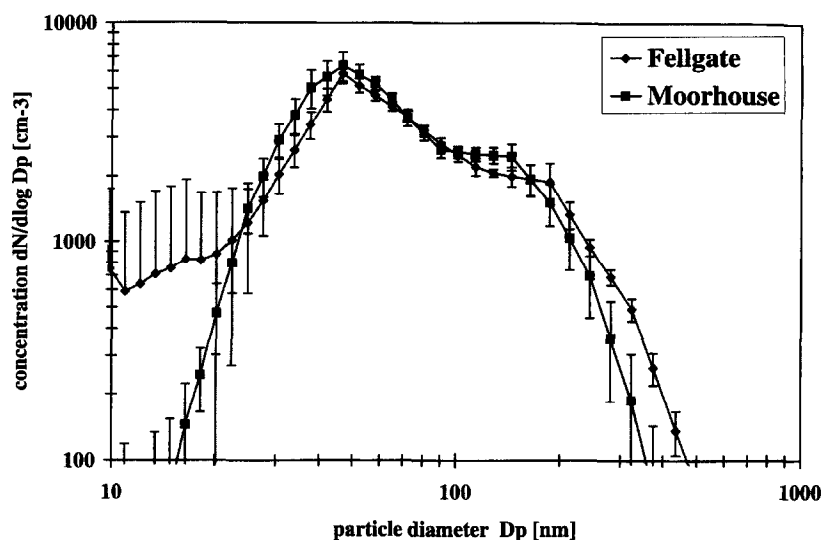


Fig. 6. Comparison of the observed DMPS aerosol spectra at MH and FG averaged over a 2 h period during case study 5. Error bars indicating + and -1 standard deviation in aerosol number are also plotted.

May 10, 22:30-23:30

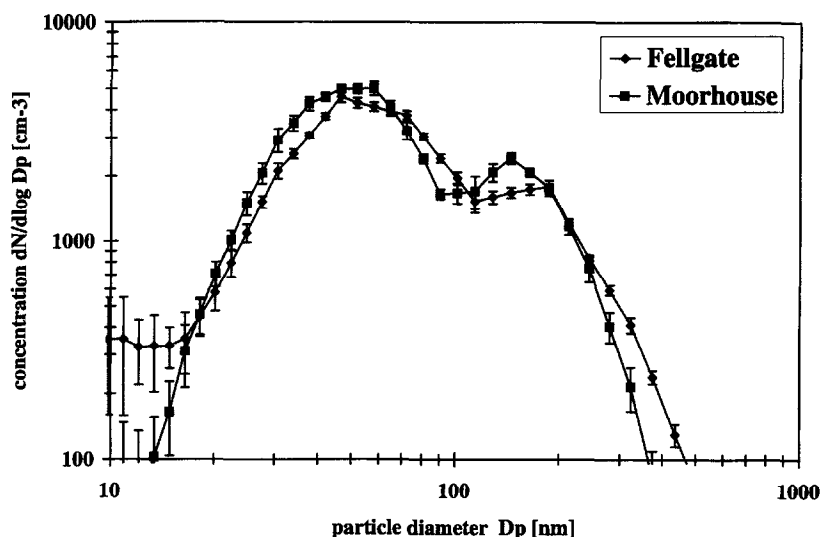


Fig. 7. As Fig. 6 but for case study 6.

strong supersaturation peaks near to cloud base. Unlike case 5, these particles remain activated for a long time, enabling a small amount of sulphate to be generated within them. The measured cloud water pH at the summit was around 4.1 during this period. The model predicted a maximum bulk cloud water pH of 4.3 at SU, falling to lower values as acidities increased at lower altitudes. The acidity was predicted to vary (by up to two pH units) across activated categories in the model, possibly enabling ozone to play a more

significant role in sulphate production in the smaller (less acidic) drops for part of their development. Although relatively small, these changes in aerosol size have a quite marked effect on the CCN activation curve of the modified aerosol (as shown in Fig. 14) increasing the number of CCN available for subsequent activation at lower cloud supersaturations. The total sulphate mass gain ($0.06 \mu\text{g m}^{-3}$) predicted by the model is too small to be detected by the impactors. However, as in case 5, the observed

May 10, 19:00-21:00

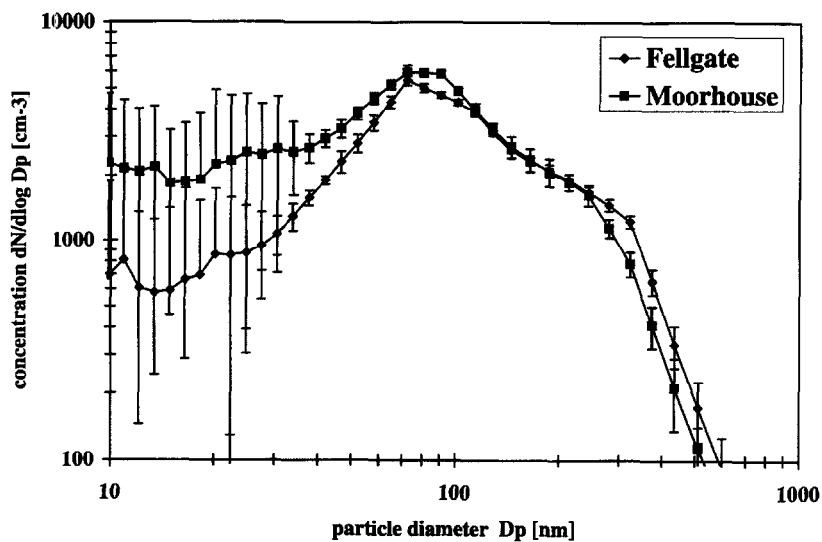


Fig. 8. As Fig. 6 but for case study 8.

May 10, 22:30-23:30

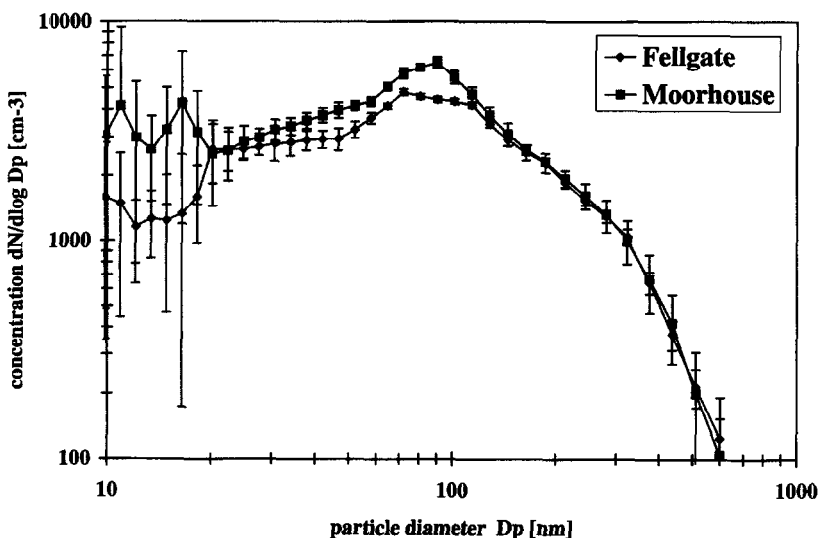


Fig. 9. As Fig. 6 but for case study 9.

modification of larger AC mode particles (300–400 nm) is inconsistent with the low SO_2 concentrations measured and used as input.

With high ambient concentrations of SO_2 present in cases 8 and 9 (4 and 6 ppbv, respectively) a substantial increase in aerosol sulphate loading is both predicted and observed. Predicted increases were 2.5 and $2.6 \mu\text{g m}^{-3}$, respectively, compared to observed increases of 2.2 and $3 \mu\text{g m}^{-3}$. During the period encompassing these runs the measured summit cloud water pH was around 3.6 and so O_3 is not expected to

have made a significant contribution to sulphate production. Again, modelled pH's of the bulk cloud water were highest at the summit and at pH 3.7 and 3.5 for runs 8 and 9, respectively, are comparable with the observed values. The predicted modification of the AC mode is much larger in these cases (e.g. see Fig. 12 for case 8), and reproduces quite well the increase in the number of large AC mode particles observed in case 8 (Fig. 8). However, the observed AC mode shows little modification in case 9, again in direct contradiction with the observed increase in sulphate and the

Run 5 (05091822)

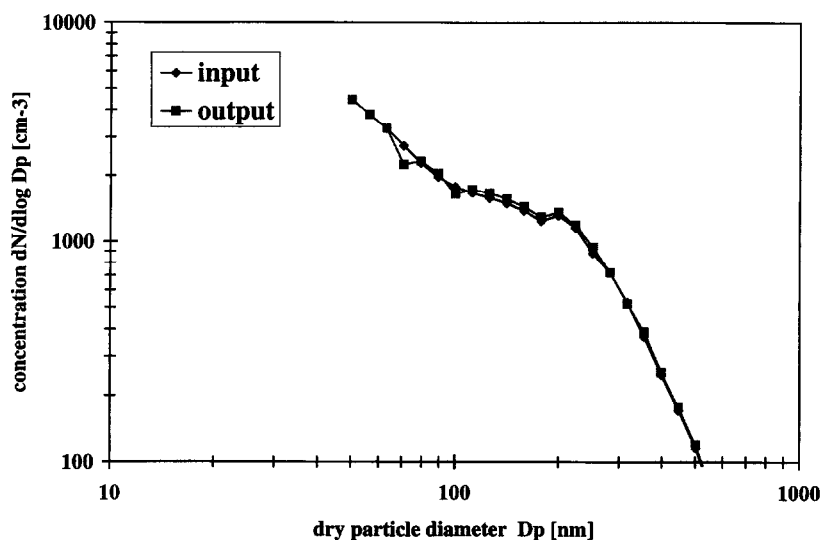


Fig. 10. The modification of the dry aerosol spectrum predicted for case study 5.

Run 6 (05100204)

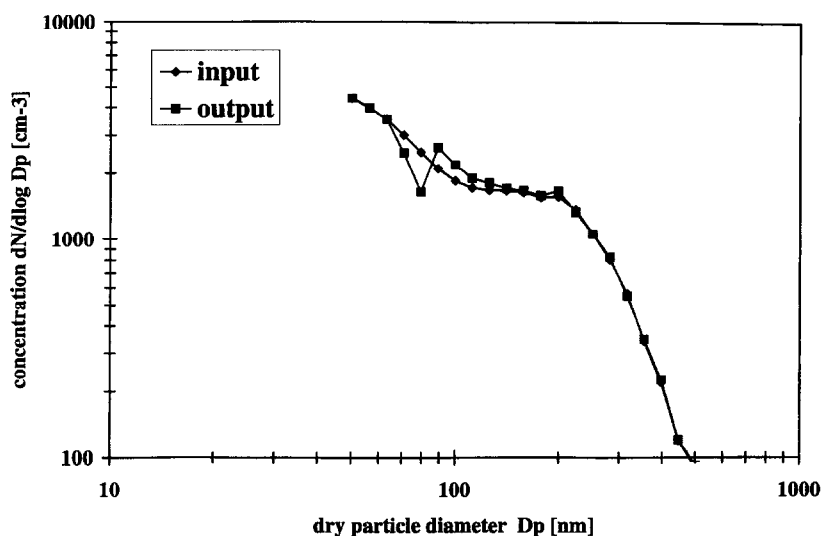


Fig. 11. As Fig. 10 but for case study 6.

high SO_2 concentrations. However, during both cases 8 and 9 there is evidence to suggest that entrainment was taking place at the summit. The liquid water content at MR was up to 33% lower than the adiabatic value expected and the ozone concentration (in L dips) was higher at MR than at SU. The SU droplet spectrum was also bimodal indicating recent (re)activation of CCN just prior to the SU. Although we have little idea of the aerosol size distribution in the tropospheric air being entrained, a comparison of the number of aerosol contained within the AK

modes upwind and downwind of the cloud (together with an estimation of the volume of entrained air from L depletion, knowing the mixing ratio of the entrained air from soundings) suggests that the entrained air is poor in aerosol number, and that entrainment is diluting the distributions within the cloud-processed air mass. If we normalise the FG AK mode number to the MH value, and apply a similar correction across the whole DMPS size range, then this in fact does lead to a modification of the AC mode consistent with the production of sulphate.

Run 8 (05101921)

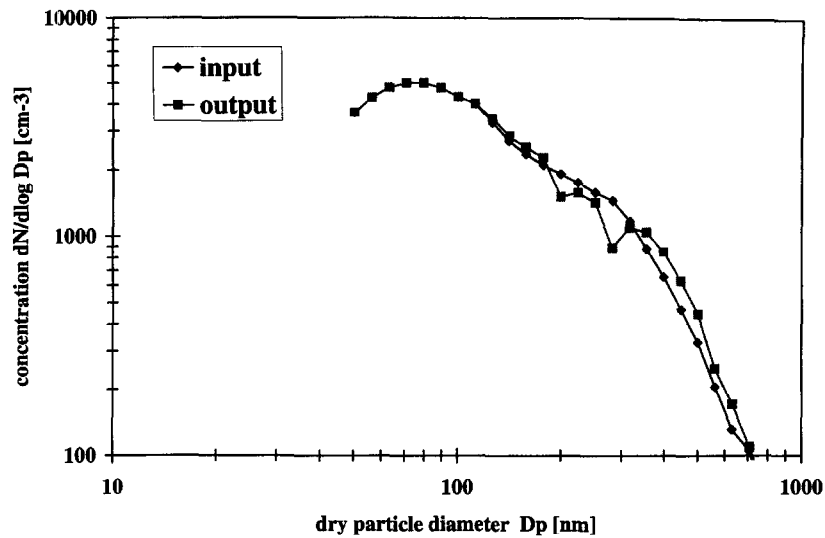


Fig. 12. As Fig. 10 but for case study 8.

Run 9 (05102323)

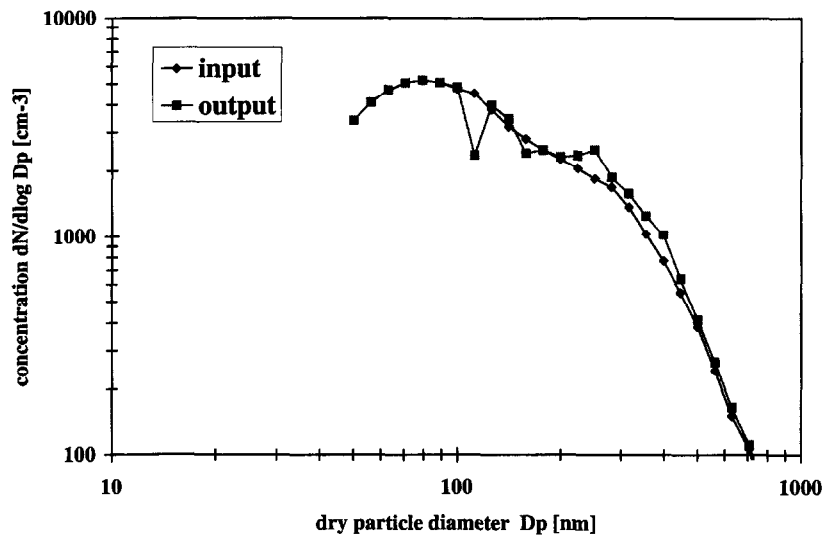


Fig. 13. As Fig. 10 but for case study 9.

In case 8, an attempt was made to compare directly the observed and modelled accumulation mode aerosol growth. A time history of the observed mean accumulation mode diameter in the approximate size range 200–600 nm shows typical growth of the AC mode (nucleation scavenged by the cloud) of between 10 and 25 nm during this period. The predicted growth in this size range was calculated to be around 20 nm.

The effect of increased sulphate production in cases 8 and 9 was expected to modify CCN properties of the

nucleation scavenged aerosol in favour of increasing the number of CCN able to subsequently activate at lower supersaturations (as in case 6, Fig. 14). However, close examination of the CCN activity curves (e.g. Fig. 15 for case 8) shows this not to be the case, except at very low cloud supersaturations S ($< 0.1\%$ for case 8 and $< 0.2\%$ for case 9). At higher S , the number of CCN able to activate is in fact reduced by the cloud processing. The smallest aerosols nucleation scavenged by cloud in these cases are predicted to lose soluble material (ammonia and HNO_3) by outgassing.

Run 6 (05100204)

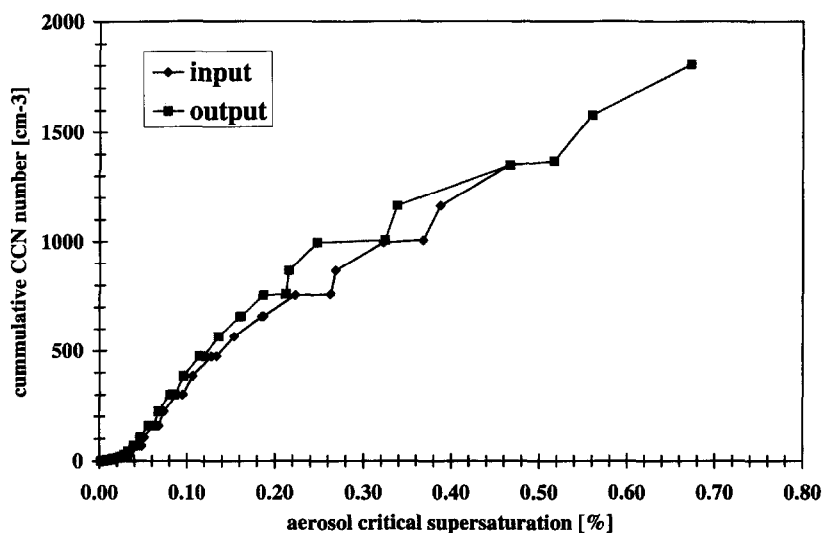


Fig. 14. The modification of the CCN activity curve predicted by the model for case study 6.

Run 8 (05101921)

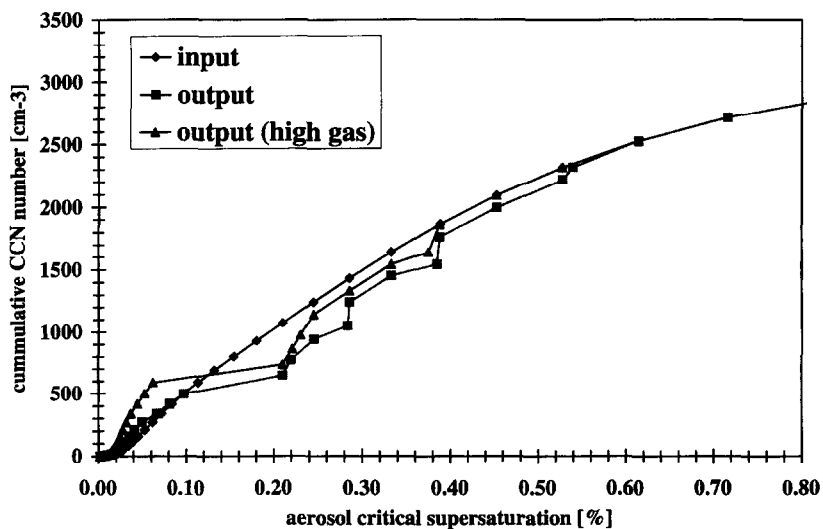


Fig. 15. As Fig. 14 but for case study 8. High gas refers to sensitivity run with 2 ppbv NH_3 and HNO_3 at input.

This is encouraged by sulphate production in the larger drops, which take up additional ammonia in order to neutralise increased acidity. The outgassing from the smallest aerosol is largest in case 9 (not shown), where these aerosol are nucleation-scavenged close to cloud base, and where the rate of sulphate production is highest in the large drops. In sensitivity tests, the degree of this outgassing was reduced by specifying high input concentrations of NH_3 and HNO_3 , or by reducing levels of the oxidant H_2O_2 , or by reducing the nitrate loading of the input aerosol.

This suggests that part of the outgassing may be attributable to a lack of information regarding the exact partitioning of nitrate between the gas and aerosol phases at input (i.e. near CB). However, Wells *et al.* (1997) also report cases where NH_3 outgassing after cloud processing was observed and measurable.

In case 8, Fig. 3 shows that the smallest aerosol activate just before the summit. It was considered that the effect of entraining hydrogen peroxide into cloud at the SU might lead to sulphate gain in these drops, offsetting the effects of outgassing. However, in the

entrainment run carried out for case 8, the smallest drops are already seen to be evaporating by the time the increased H_2O_2 has any significant effect. The entrainment of fresh oxidant leads only to an increase in sulphate within the largest drops during the descent to cloud base, and so has little additional effect upon the CCN spectrum. No entrainment of aerosol into the cap cloud was assumed during these runs.

4. DISCUSSION

It has been shown that an aerosol size distribution can be substantially modified by passage through a cloud system. In the case studies examined, the source of the modification was generally found to be related to the in-cloud production of sulphate either directly or indirectly. When entrainment was occurring through the cloud top, the effect of introducing air which was assumed to have a lower aerosol number concentration, was to dilute the aerosol distribution emerging from the cloud system. In one example, this was seen to obscure the effects of in-cloud sulphate production within aerosol activated at cloud base.

The model results suggest that in order to increase significantly the number of large accumulation mode particles present in a distribution, a large conversion of SO_2 to sulphate is required. In different conditions the scavenging of other gas-phase species such as oxides of nitrogen and HNO_3 will also be important (particularly in the presence of ammonia gas), having a similar effect of adding soluble material to the CCN mass already present within nucleation-scavenged aerosol. This will significantly modify the direct radiative properties of the processed aerosol distribution. However, adding soluble mass to nucleation-scavenged aerosol will have little effect on the indirect radiative properties of aerosol (i.e. their ability to act as CCN) if only the large aerosol are affected. These are already efficient CCN and a small fractional increase in their soluble mass (which when integrated may add up to a considerable increase in the total soluble mass loading of the aerosol) will not significantly reduce the already low supersaturations required for them to reactivate to form cloud drops.

In order to modify significantly the indirect radiative properties of aerosols, the changes brought about by cloud processing have to occur within the smallest activated aerosol. Here, even a very small change in the total soluble mass loading of the aerosol distribution can substantially change the capacity of the smallest nucleation scavenged aerosol to act as CCN. This study has shown that the modification of the aerosol size distribution at sizes smaller than the large accumulation mode particles is a considerably more complex issue. Such modification is seen to be dependent upon a number of factors which include, the activation history of the nucleation scavenged aerosol, the ambient level of pollutant gases, the de-

gree of sulphate production and the time at which this occurs in-cloud, as well as the external mix of the aerosol chemical composition (discussed here and by others e.g. Yuen *et al.*, 1994) which can lead to differential chemistry and/or repartitioning of species between drop categories.

The supersaturation histories of clouds at GDF in 1993 were complex when the wind was blowing from the NE, as evidenced by the breadth and shape of droplet size distributions observed at the summit. The model, which is able to reproduce the main observed features of the cloud, suggests that the S histories experienced are strongly dependent upon the wind speed and the exact trajectory followed by parcels to the hill summit.

When sulphate production occurs, the addition of soluble material to the smallest activated aerosol is favoured by a simple activation history which is non-staggered (and for the aerosol inputs used in this paper which may not all have been in equilibrium with the gas phase at input, by having a short transit time through the processing cloud, i.e. a high cloud base). This will cause the peak supersaturation to occur near cloud base, enabling activation of the smallest CCN early on (at around the same time as the majority of the cloud droplet population), their growth by sulphate production, and a minimum of interference from the larger droplet systems during the lifetime of the cloud parcel. Sulphate production in these circumstances can lead to a substantial increase in the number of CCN able to activate at much lower supersaturations in subsequent clouds, even if the level of sulphate production is not high (e.g. as in the extreme example of model run 6).

In conditions where the gas-phase concentration of SO_2 is very high and there is little NH_3 present in the ambient air, with adequate levels of oxidant available the effect of strong sulphate production within the largest aerosols can be to cause a loss of ammonium from the smallest activated CCN. In these circumstances, the larger drops rapidly remove as much NH_3 from the gas-phase as possible in order to neutralise the high-level acidities accompanying sulphate production. The depletion of gas-phase ammonia encourages the smaller drops to outgas ammonia, reducing both sulphate production and the mass of ammonium present in these drops. If these activated aerosols contain salts of volatile acids (such as HNO_3), these may also outgas in order to reduce acidity. This outgassing will be enhanced if the aerosols entering the cloud system are not in equilibrium with the gas-phase concentrations of NH_3 (and HNO_3) near cloud base. This scenario can lead to modified aerosol spectra in which there is both an increase in the size of the largest aerosol (these would be able to activate at a slightly lower S than before) but a reduction in the number of CCN able to activate in a subsequent cloud with peak supersaturation values similar to those of the processing cloud system. This appeared to be the resultant effect in case study 8 (and 9 if the effects of

aerosol dilution due to entrainment are taken into account) where outgassing was predicted and the exact nitrate loading of the dry input aerosol could not be determined. This CCN modification is obviously favoured by the smallest aerosol remaining activated for as long as possible during their transit through cloud.

It is suggested that in the absence of observable sulphate production, significant CCN modification might still arise as a result of cloud processing under certain circumstances. This modification could be brought about by the repartitioning of material either between the aerosol and gas-phase or between aerosols of different initial size and composition. The addition of soluble mass by the scavenging of gases such as the oxides of nitrogen and HNO_3 has already been discussed, as has the outgassing of CCN species and repartitioning during sulphate production. However, the latter processes may also occur in the absence of any S(IV) oxidation. This was highlighted during sensitivity studies for the case study model runs presented. Outgassing was observed to take place from all categories in the presence of low gas-phase concentrations of pollutants during long in-cloud transits. Repartitioning between aerosols of different composition and size was also observed during these periods. Again the effects are most noticeable when the smallest activated CCN are involved.

Entrainment of heat and fresh oxidant was not observed to have a large effect on CCN modification in the case studies 8 and 9 modelled (during which entrainment was observed). Previous observations suggest entrainment is at its maximum at cloud top near to the summit, and so its effects are mainly detected downwind of this. Since most small drops are evaporating rapidly by this stage (even if more were recently activated close to the summit), they are unable to make use of the fresh oxidant introduced. The additional burst of sulphate production is thus contained within the larger drops formed on the largest CCN. The activation curve of the modelled aerosol is thus unchanged as a result of entrainment. Observations of the number concentration of AK mode particles present in the aerosol spectra of cases 8 and 9 suggest that, entrainment may be showing up as a dilution effect (due to the entrained air containing fewer aerosol particles). In case 9, this appears to have completely obscured the effects of adding sulphate to the aerosol activated at or near cloud base. However, since no measurements of the tropospheric aerosol were made, a quantitative study of the effects of entrainment on the modification of the aerosol is difficult to undertake for this experiment.

Acknowledgements—Funding for this experiment and related work was provided by the following agencies: The UK Department of Environment (Contract PEC07/12/32), the Commission of the European Union (Contract EV5V-CT94-0450), the U.K. Natural Environment Research Council, the Ministry of Economic Affairs of The Netherlands, Austrian Fonds zur Förderung der Wissenschaftlichen Forschung

(Project P09740TEC), Bundesministerium für Bildung und Forschung (Project 07EU773-07EU773/A6), the Swedish Environment Protection Board, the Swedish Council for Planning and Coordination of Research, the Swedish Natural Science Research Council and the Swedish National Board for Technical Development. The Environment Program of the European Commission DG XII provided travel grants for GCE participants to meet and discuss the results of the present experiment. The Great Dun Fell Cloud Experiment 1993 was carried out within the EUROTRAC subproject GCE (Ground-based Cloud Experiment).

REFERENCES

- Bower, K. N. and Choulaton, T. W. (1988) The effects of entrainment on the growth of droplets in continental cumulus clouds. *Q. Jl. R. Met. Soc.* **114**, 1411–1434.
- Bower, K. N. and Choulaton, T. W. (1993) Cloud processing of the cloud condensation nucleus spectrum and its climatological consequences. *Q. Jl. R. Met. Soc.* **119**, 655–680.
- Bower, K. N., Hill, T. A., Coe, H. and Choulaton, T. W. (1991) Sulphur dioxide oxidation in an entraining cloud model with explicit microphysics. *Atmospheric Environment* **25A**, 2401–2418.
- Charlson, R. J., Schwartz, S. E., Hales, J. M., Cess, R. D., Coakley, J. A. Jr., Hansen, J. E. and Hofmann, D. J. (1992) Climate forcing by anthropogenic aerosols. *Science* **255**, 423–430.
- Choulaton, T. W., Colvile, R. N., Bower, K. N., Gallagher, M. W., Wells, M., Beswick, M. W., Arends, B. G., Möls, J. J., Kos, P. A., Fuzzi, S., Lind, J. A., Orsi, G., Facchini, M. C., Laj, P., Gieray, R., Wieser, P., Engelhardt, T., Berner, A., Krusiz, C., Moller, D., Acker, A., Wiprecht, W., Luttke, J., Levens, K., Bizjak, M., Hansson, H.-C., Cederfelt, S.-I., Frank, G., Mentes, D., Martinsson, B., Orsini, D., Svenningsson, B., Swietlicki, E., Wiedensohler, A., Noone, K. J., Pahl, S., Winkler, P., Seyffer, E., Helas, G., Jaeschke, W., Georgii, H. W., Wobrock, W., Preiss, M., Maser, R., Schell, D., Dollard, G., Jones, B., Davies, T., Sedlak, D. L., David, M. M., Wendisch, M., Cape, J. N., Hargreaves, K. J., Sutton, M. A., Storeton-West, R. L., Fowler, D., Hallberg, A., Harrison, R. M. and Peak, J. D. (1997) The Great Dun Fell Cloud experiment 1993: An overview. *Atmospheric Environment* **31**, 2393–2405.
- Colvile, R. N., Sander, R., Choulaton, T. W., Bower, K. N., Inglis, D. W. F., Wobrock, W., Maser, R., Schell, D., Svenningsson, I. B., Wiedensohler, A., Hansson, H.-C., Hallberg, A., Ogren, J. A., Noone, K. J., Facchini, M. C., Fuzzi, S., Orsi, G., Arends, B. G., Winiwater, W., Schneider, T. and Berner, A. (1994) Computer modelling of clouds at Kleiner Feldberg. *J. Atmos. Chem.* **19**, 189–229.
- Colvile, R. N., Bower, K. N., Choulaton, T. W., Gallagher, M. W., Wobrock, W., Hargreaves, K. J., Storeton-West, R. L., Cape, J. N., Jones, B., Wiedensohler, A., Hansson, H.-C., Wendisch, M., Acker, K., Wiprecht, W., Pahl, S., Winkler, P., Berner, A. and Krusiz, C. (1997) Meteorology of the Great Dun Fell Cloud Experiment 1993. *Atmospheric Environment* **31**, 2407–2420.
- Gallagher, M. W., Choulaton, T. W., Downer, R. M., Tyler, B. J., Stromberg, I. M., Mill, C. S., Penkett, S. A., Bandy, B., Dollard, G. J., Davies, T. J. and Jones, B. M. R. (1991) Measurements of the entrainment of hydrogen peroxide into cloud systems. *Atmospheric Environment* **25A**, 2029–2038.
- Hallberg, A., Wobrock, W., Flossmann, A. I., Bower, K. N., Wiedensohler, A., Hansson, H.-C., Wendisch, M., Berner, A., Krusiz, C., Laj, P., Facchini, M. C., Fuzzi, S. and Arends, B. G. (1997) Microphysics of clouds: model versus measurements. *Atmospheric Environment* **31**, 2453–2462.

- Hill, T. A., Choulaton, T. W. and Penkett, S. A. (1986) A model of sulphate production in a cap cloud and subsequent turbulent deposition onto the hill surface. *Atmospheric Environment* **20**, 1763–1771.
- Hoppel, W. A., Frick, G. M. and Fitzgerald, J. W. (1994) Marine boundary layer measurements of new particle formation and the effects nonprecipitating clouds have on aerosol size distribution. *J. geophys. Res.* **99**, 14,443–14,459.
- Laj, P., Fuzzi, S., Facchini, M. C., Orsi, G., Berner, A., Krusiz, C., Wobrock, W., Hallberg, A., Bower, K. N., Gallagher, M., Beswick, K. M., Colvile, R. N., Choulaton, T. W., Nason, P. and Jones, B. (1997) Experimental evidence for in-cloud production of aerosol sulphate. *Atmospheric Environment* **31**, 2503–2514.
- Pruppacher, H. R. and Klett, J. D. (1978) *Microphysics of Clouds and Precipitation*. D. Reidel, London.
- Sander, R., Lelieveld, J. and Crutzen, P. (1995) Model calculations of the nighttime chemistry of nitrogen and sulfur compounds in size resolved droplets of an orographic cloud. *J. atmos. Chem.* **20**, 89–116.
- Shulman, M. L., Jacobson, M. C., Charlson, R. J., Synovec, R. E. and Young, T. E. (1996) Dissolution behaviour and surface tension effects of organic compounds in nucleating cloud droplets. *Geophys. Res. Lett.* **23**, 277–280.
- Slingo, A. (1990) Sensitivity of the Earth's radiation budget to changes in low clouds. *Nature* **343**, 49–51.
- Svenningsson, B., Hansson, H.-C., Martinsson, B., Wiedensohler, A., Swietlicki, E., Cederfelt, S.-I., Wendisch, M., Bower, K. N., Choulaton, T. W. and Colvile, R. N. (1997) Cloud droplet nucleation scavenging in relation to the size and hygroscopic behaviour of aerosol particles. *Atmospheric Environment* **31**, 2463–2475.
- Wells, M., Bower, K. N., Choulaton, T. W., Cape, J. N., Sutton, M. A., Storeton-West, R. L., Fowler, D., Wiedensohler, A., Hansson, H.-C., Svenningsson, B., Swietlicki, E., Wendisch, M., Jones, B., Dollard, G., Acker, K., Wieprecht, W., Preiss, M., Arends, B. G., Pahl, S., Berner, A., Krusiz, C., Laj, P., Facchini, M. C. and Fuzzi, S. (1997) The reduced nitrogen budget of an orographic cloud. *Atmospheric Environment* **31**, 2599–2614.
- Wiedensohler, A., Hansson, H.-C., Orsini, D., Wendisch, M., Wagner, F., Bower, K. N., Choulaton, T. W., Wells, M., Parkin, M., Acker, K., Wieprecht, W., Facchini, M. C., Lind, J. A., Fuzzi, S. and Arends, B. G. (1997) Night-time formation of new particles associated with orographic clouds. *Atmospheric Environment* **31**, 2545–2559.
- Wobrock, W., Flossmann, A. I., Colvile, R. N. and Inglis, D. W. F. (1997) Modelling of airflow and cloud fields over the northern Pennines. *Atmospheric Environment* **31**, 2421–2439.
- Yuen, P. F., Hegg, D. A. and Larson, T. V. (1994) The effects of in-cloud sulfate production on the light scattering properties of continental aerosol. *J. appl. Met.*, **33**, 848–854.